Received: 14 June 2019 | Revised: 13 July 2019 | Accepted: 6 August 2019

DOI: 10.1111/aor.13556

MAIN TEXT ARTICLE

Artificial Organs WILEY

A strategy for designing of customized electromechanical actuators of blood pumps

Rogerio Lima de Souza[1] | **Ivan Eduardo Chabu**[2] | **Evandro Drigo da Silva**[1,3] | **Aron Jose Pazin de Andrade**[3] | **Tarcisio Fernandes Leao**[1,3] | **Eduardo Guy Perpetuo Bock**[1,3]

[1]Laboratory of Bioengineering and Biomaterials BIOENG, Department of Mechanics, Federal Institute of Technology in Sao Paulo IFSP, Sao Paulo, Brazil

[2]Laboratory of Applied Electromagnetism LMAG, Department of Electrical Engineering, Escola Politecnica EPUSP, University of Sao Paulo, Sao Paulo, Brazil

[3]Center for Engineering in Cardiac Assistance CEAC, Institute Dante Pazzanese of Cardiology IDPC, Sao Paulo, Brazil

Correspondence
Rogerio Lima de Souza, Laboratory of Bioengineering and Biomaterials BIOENG, Department of Mechanics, Federal Institute of Technology in Sao Paulo IFSP, Av. Alto do Parnaiba 491 Cidade Patriarca, Sao Paulo 03556-030, Brazil.
Email: srogerio.limas@gmail.com

Funding information
Coordenação de Aperfeiçoamento de Pessoal de Nível Superior, Grant/Award Number: PGPTA 88887.123938/2014-00; Fundação de Amparo à Pesquisa do Estado de São Paulo, Grant/Award Number: PIPE/PITCHGOV 2017/25233-9; Conselho Nacional de Desenvolvimento Científico e Tecnológico, Grant/Award Number: 310085/2015-2

Abstract

Congestive heart failure is a pathology of global incidence that affects millions of people worldwide. When the heart weakens and fails to pump blood at physiological rates commensurate with the requirements of tissues, two main alternatives are cardiac transplant and ventricular assist devices (VADs). This article presents the design strategy for development of a customized VAD electromagnetic actuator. Electromagnetic actuator is a brushless direct current motor customized to drive the pump impeller by permanent magnets located in rotor–stator coupling. In this case, ceramic pivot bearings support the VAD impeller. Electronic circuitry controls rotation switching current in stator coils. The proposed methodology consisted of analytical numerical design, tridimensional computational modeling, numerical simulations using Maxwell software, actuator prototyping, and validation in the dynamometer. The axial flow actuator was chosen by its size and high power density compared to the radial flow type. First step consisted of estimating the required torque to drive the pump. Torque was estimated at 2100 rpm and mean current of 0.5 A. Numerical analysis using finite element method mapped vectors and fields to build stator coils and actuator assemblage. After tests in the dynamometer, experimental results were compared with numerical simulation and validated the proposed model. In conclusion, the proposed methodology for designing of VAD electromechanical actuator was considered satisfactory in terms of data consistency, feasibility, and reliability.

KEYWORDS
brushless direct current motor, computational numerical simulation, electromagnetic actuator, implantable centrifugal blood pump, ventricular assist device

1 | INTRODUCTION

Congestive heart failure is a pathology of global incidence that affects more than 20 millions of people worldwide. It is largely categorized and consists of a progressive clinical state when the heart weakens and fails to pump blood at physiological rates commensurate with the requirements of tissues. Thus, two main alternatives for treatment are cardiac transplant and therapies associated with ventricular assist devices (VADs).[1,2]

The implantable centrifugal blood pump (ICBP) is a VAD for long-term assistance initially designed for bridge to transplant (BTT) in conjunction with several research institutions.[3,4]

Actuators are important for the performance of blood pumps and are intrinsically connected to the operation of the equipment. Several topologies have been proposed over the years in area of artificial organs and VADs.[5–14]

This article presents a design strategy for development of a customized electromagnetic actuator for ICBP elaborated after more than 10 years of technique enhancement.[15] Electromagnetic actuator is a brushless direct current motor customized to drive the pump impeller by permanent magnets located in rotor–stator coupling.[16,17] In this case, ceramic pivot bearings support the VAD impeller. Electronic circuitry controls rotation switching current in stator coils.[18–21]

2 | MATERIALS AND METHODS

The proposed methodology for a customized design of electromechanical actuator consisted of analytical numerical design, tridimensional computational modeling, numerical simulations using Maxwell software, actuator prototyping, and validation in a dynamometer.

Based on the data obtained during previous hydrodynamic performance tests,[15] torque was estimated analytically from estimated pump power and pump output at 2100 rpm and mean current of 0.5 A. Figure 1 shows coil dimensions based on rotor dimensions and magnetic properties such as remnant magnetization and coercive force.[22,23]

Starting from the adopted current density of 3.10^6 A/m^2, with conductor diameter of 4.6×10^{-4} m, relative magnet permeability of 1.12, and magnetic flux density of 8.4×10^{-1} T, the number of turns per coil was calculated in 50 turns as seen in Equation 1.

$$N_{\mathrm{ph}} = \frac{2 \times \pi \times T_{\mathrm{n}}}{B_{\mathrm{mg}} \times m_{\mathrm{fase}} \times I_{\mathrm{rms}} \times N_{\mathrm{p}} \times d_{\mathrm{i}}^2} \quad (1)$$

In order to make the computational numerical analysis by finite element method, the prototype was modeled (Inventor, Autodesk, San Rafael, CA, USA) and exported (Maxwell 3D, ANSYS, Canonsburg, PA, USA).

A dynamometer designed by the research group[24] measured torque of the assembled rotor–stator configuration to compare and validate the computational numerical simulation results.

3 | RESULTS

Figure 2 shows the tridimensional model design and the results for density of magnetic flux in rotor represented by vectors obtained after numerical simulation. Permanent magnets with positive poles are in red and negative poles in blue. Vectors followed the expected magnetic field lines.[17]

The interaction between magnetic poles evidenced small vectors with lower magnitude and different orientations. The values obtained in the actuator simulation and the magnetic flux density were compared with the theoretically calculated value B_{avg}.[16] Figure 3 shows the numerical simulations of the proposed actuator, with three groups of coils, A in blue, B in yellow, and C in purple.

The torque calculated by the software was compared with the experimental value of torque measured in the dynamometer. Figure 4 shows the torque generated by the proposed actuator in the numerical simulation as a function of the angular position. The graph shows peaks because the variation from 0° to 360° was determined with a pitch of 60° polar pitch, with a maximum value of 9.3 mNm.

After first characterization, coils were manually rolled. A device was created with the rolling profile as shown in Figure 5A, to give the desired trapezoidal shape and control the external dimensions of the coil (B). A template (C) was applied to control the same geometric characteristics in coils.

After this process, coils were identified and welded in series by groups A, B, and C. Each phase is composed of three coils encased in epoxy resin. Figure 6 shows the complete stator with encased coils and three wires soldered for phase feed with terminal connectors.

The assembled dynamometer measured torque and mechanical power to validate numerical simulations and analytical calculation.[25–29] Figure 7 shows the experimental setup.

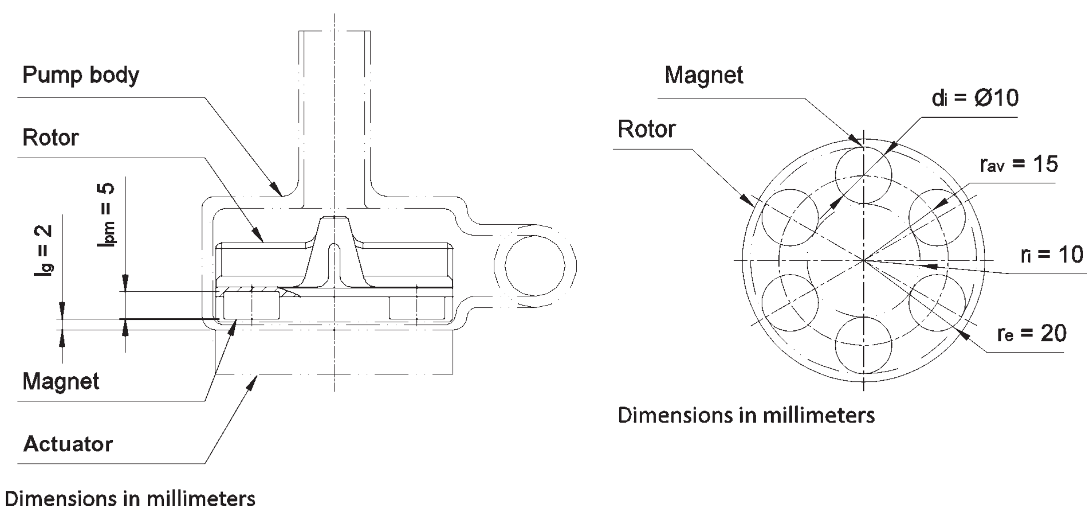

FIGURE 1 VAD schematics showing pump, impeller and actuator, magnets and dimensions

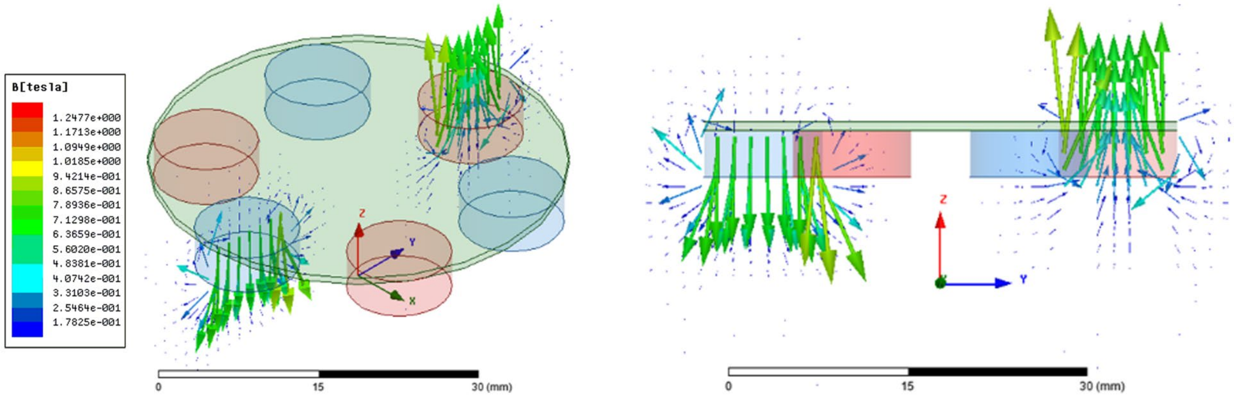

FIGURE 2 Tridimensional model and the density of magnetic flux in rotor obtained after numerical simulations [Color figure can be viewed at wileyonlinelibrary.com]

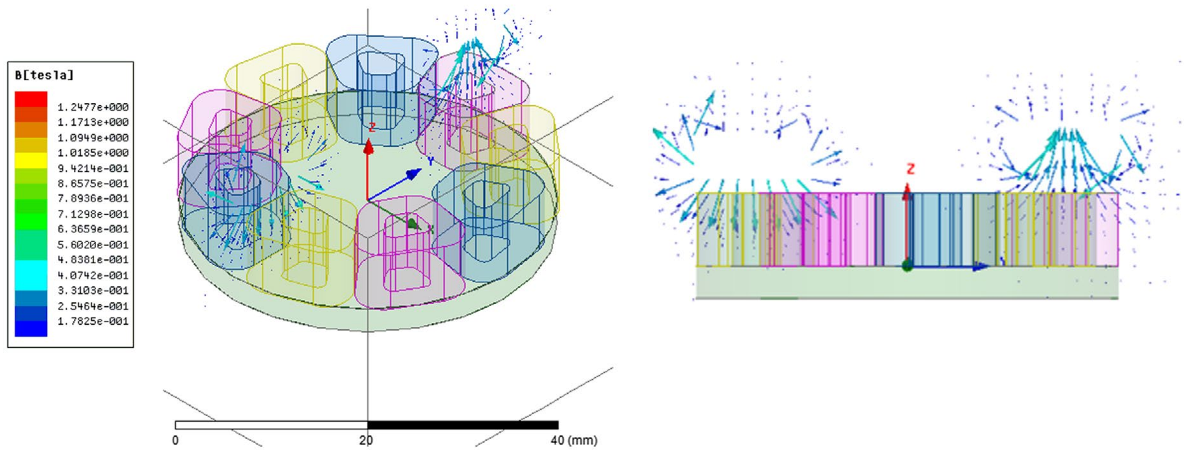

FIGURE 3 Coil design and the density of magnetic flux in stator obtained after numerical simulations [Color figure can be viewed at wileyonlinelibrary.com]

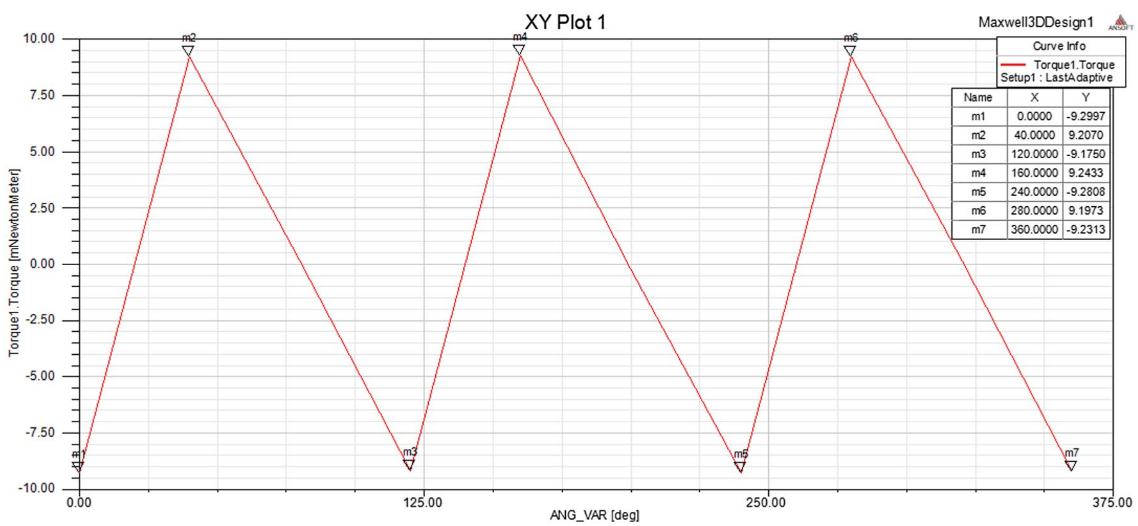

FIGURE 4 Torque generated by actuator and its variation from 0° to 360° with a 60° polar pitch [Color figure can be viewed at wileyonlinelibrary.com]

Indicator (A) has two displays for torque generated by actuator (B) and axial force (C) with respective scale selector switches. Display (B) has two scale options, 25 and 100 mN.m, and the display (C) has two options 25 and 100 N scale options. Voltage and current were obtained from power supply panel (D) and measured in controller board input (E). Digital tachometer

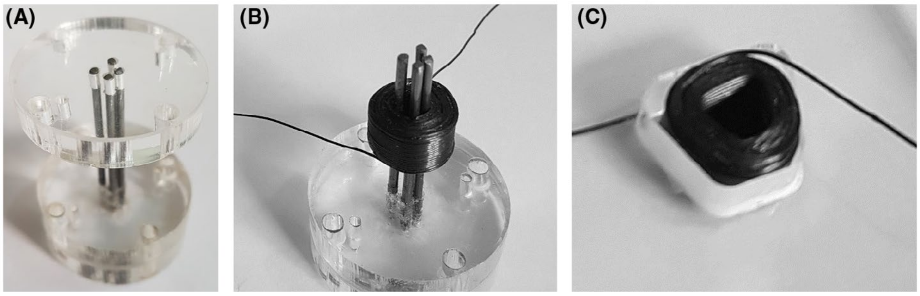

FIGURE 5 Device (A) used for manually winding actuator coils (B) and a template to control dimensions and required trapezoidal profile (C)

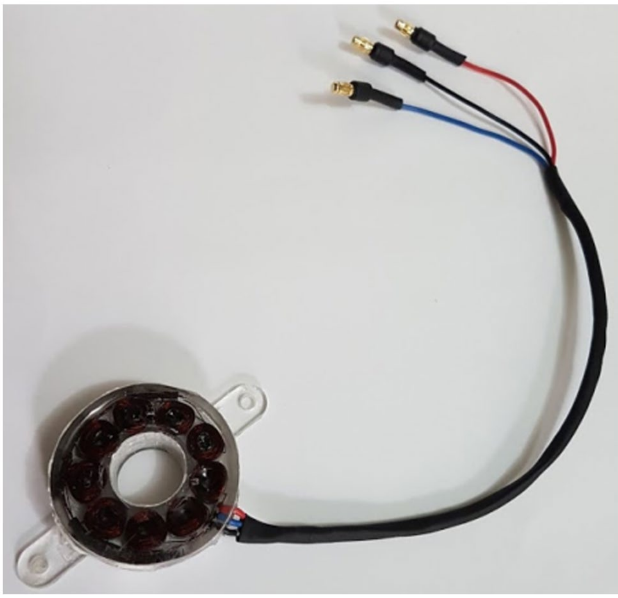

FIGURE 6 Complete stator with wires and terminals [Color figure can be viewed at wileyonlinelibrary.com]

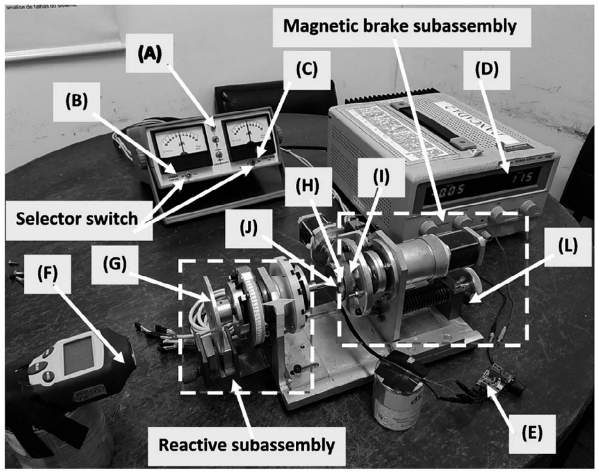

FIGURE 7 Experimental setup with assembled dynamometer and mounted actuator

TABLE 1 Mounted actuator characteristics measured by dynamometer in the experimental setup

Actuator characteristics – l_g = 2 [mm]						
Main Voltage in power supply 12 [V]						
V_f [V]	I_f [mA]	n [rpm]	C [mN m]	W_{abs} [W]	W_{mec} [W]	η [%]
11.60	1290	3505.30	4.00	14.96	1.47	9.81
12.00	1360	3134.10	5.00	16.32	1.64	10.06
12.00	1400	2005.00	6.00	16.80	1.26	7.50
12.10	1490	1520.00	8.00	18.03	1.27	7.06
12.10	1530	735.90	9.00	18.51	0.69	3.75
12.00	1620	529.60	11.00	19.44	0.61	3.14

(F) was positioned to measure revolutions of the magnetic brake disk (G). Actuator (H) and adapter plate (I) were mounted on the dynamometer reactive subassembly, which measures reactive torque (J) on the magnetic brake subassembly. It applies a restrictive load on the rotor allowing speed variation. Air gap is adjusted by screw (L) as specified in the design.[24,26]

4 | DISCUSSION

As seen in Table 1, data were obtained in function of rotation. In order to vary rotation, mechanical load was applied with the magnetic brake until rotation stabilizes and all data could be recorded.

Thus, successively, the load was applied gradually with the magnetic brake. Variables W_{abs} absolute power, W_{mec} mechanical power, and "η" yield were calculated with the data collected.

5 | CONCLUSIONS

Analytically estimated torque was 10×10^{-3} N·m. Based on this result, torque was increased by 20% with operating range, already operating current and rotor dimensions already established. Parameters adopted were torque 12×10^{-3} N·m, rotation range 2100 rpm and a mean current of 0.5 A. With these parameters, it was possible to calculate the number of turns required per phase.

Then, a numerical analysis was performed by finite element method, which had values obtained by the analytical calculation as input data. Maximum torque was calculated by the software as 9.3×10^{-3} N·m.

Finally, the actuator was machined, prototyped, and tested in the dynamometer to survey its characteristic curves. These experimental values were compared with numerical simulations to validate them. Efficiency was considered relatively low as expected due to manual windings manufacturing that increases resistance in coils, temperature, and current consumption. Finally, analyzing computational data with experimental data, the conclusion is that the actuator has expected torque for the chosen rotation range and the proposed design strategy for VAD actuator was successful.

After validating the computational model, analyzing results obtained through computational simulation, and comparing dynamometer measurements, it is possible to state that the applied design strategy can be extrapolated to several types of centrifugal pumps applied as blood pumps and VADs. As observed in many devices, the application of custom motors can provide improvements in performance and reliability, ensuring application safety and patients' health.

ACKNOWLEDGMENTS

This work was only possible with financial funding of CAPES, CNPq, and FAPESP. Authors acknowledge Brazilian Funding Agencies CAPES PGPTA 88887.123938/2014-00, CNPq 310085/2015-2, FAPESP PIPE/PITCHGOV 2017/25233-9. In addition, authors would like to thank Universidade Estadual Paulista "Júlio de Mesquita Filho" (UNESP) in Sorocoba, Sao Paulo.

CONFLICT OF INTEREST

The authors report no conflict of interest.

AUTHOR CONTRIBUTIONS

Drafting article: de Souza
Critical revision of article: Chabu, Drigo da Silva, Leao
Concept/design: de Andrade
Approval of article: Bock

ORCID

Tarcisio Fernandes Leao
https://orcid.org/0000-0003-4884-5638
Eduardo Guy Perpetuo Bock
https://orcid.org/0000-0003-3962-9052

REFERENCES

1. Gemmato CJ. Thirty-five years of mechanical circulatory support at the Texas Heart Institute: an updated overview. Texas Heart Inst J. 2005;32(2):168–77.
2. Sen A, Larson JS, Kashani KB, Libricz SL, Patel BM, Guru Pramod K, et al. Mechanical circulatory assist devices: a primer for critical care and emergency physicians. Crit Care. 2016;20(1):153.
3. Bock E, Ribeiro A, Silva M, Antunes P, Fonseca J, Legendre D, et al. New centrifugal blood pump with dual impeller and double pivot bearing system: wear evaluation in bearing system, performance tests, and preliminary hemolysis tests. Artif Organs. 2008;32(4):329–33.
4. Lopes G, Bock E, Gómez L. Analyses and grid density estimation for ventricular assist devices in multiple reference frames simulations. Technische Mechanik. 2016;36(3):190–8.
5. Mitamura Y, Wada T, Sakai R. A ferrofluidic actuator for an implantable artificial heart. Artif Organs. 1992;16:490–5.
6. Van Der Smissen B, Claessens T, Verdonck P, Van Ransbeeck P, Segers P. Design of an artificial left ventricular muscle: an innovative way to actuate blood pumps? Artif Organs. 2009;33:464–8.
7. Jeong GS, Hwang CM, Nam KW, Ahn CB, Kim HC, Lee JJ, et al. Development of a closed air loop electropneumatic actuator for driving a pneumatic blood pump. Artif Organs. 2009;33:657–62.
8. Chung J, Kim WE, Lee JJ, Nam KW, Choi J, Park JW, et al. Assessment and improvement of the system efficiency for the moving-actuator type biventricular assist device. Artif Organs. 2004;28:549–55.
9. Santos CM, Cunha FL, Dynnikov VI. The application of shape memory actuators in anthropomorphic upper limb prostheses. Artif Organs. 2003;27:473–7.
10. Min BG, Kim HC, Lee SH, Kim IY, Kim JW, Choi JW, et al. Development of a new moving-actuator type electromechanical total artificial heart. Artif Organs. 1991;15:144–6.
11. Lim TM, Cheng S, Chua LP. Parameter estimation and actuator characteristics of hybrid magnetic bearings for axial flow blood pump applications. Artif Organs. 2009;33:509–31.
12. Sasaki Y, Chikazawa G, Nogawa M, Nishida H, Koyanagi H, Takatani S. Ex vivo evaluation of a roller screw linear muscle actuator for an implantable ventricular assist device using trained and untrained latissimus dorsi muscles. Artif Organs. 1999;23:262–7.

13. Ahn JM, Lee JH, Choi SW, Kim WE, Omn KS, Park SK, et al. Implantable control, telemetry, and solar energy system in the moving actuator type total artificial heart. Artif Organs. 1998;22:250–9.
14. Kim WG, Chang JK, Kim HC, Min BG, Won YS, Rho JR. Moving Actuator Type Total Artificial Heart with Reverse Position of the Aortic and Pulmonary Conduits. Artif Organs. 1997;21:957–60.
15. Bock E, Andrade A, Dinkhuysen J, Arruda C, Fonseca J, Leme J, et al. Introductory tests to in vivo evaluation: magnetic coupling influence in. ASAIO J. 2011;57(5):462–5.
16. Hendershot JR, Miller TJ. Design of brushless permanent-magnet motors. Hillsboro, OH & Oxford: Magna Physics Publishing & Oxford University Press; 1994.
17. Gieras JF, Wang RJ, Kamper MJ. Axial flux permanent magnet brushless machines. Berlin/Heidelberg: Springer Science & Business Media; 2008.
18. Uebelhart B, Utiyama B, Fonseca J, Bock E, Leme J, Silva C, et al. Study of a centrifugal blood pump in a mock loop system. Artif Organs. 2013;37(11):946–9.
19. Fonseca J, Andrade A, Nicolosi D, Biscegli J, Legendre D, Bock E, et al. A new technique to control brushless motor for blood pump application. Artif Organs. 2008;32(4):355–9.
20. Nishida M, Maruyama O, Kosaka R, Yamane T, Kogure H, Kawamura H, et al. Hemocompatibility evaluation with experimental and computational fluid dynamic analyses for a monopivot circulatory assist pump. Artif Organs. 2009;33(4):378–86.
21. Kosaka R, Nishida M, Maruyama O, Yambe T, Imachi K, Yamane T. Effect of a bearing gap on hemolytic property in a hydrodynamically levitated centrifugal blood pump with a semi-open impeller. Bio-Medical Mat and Eng. 2013;23:37–47.
22. Batzel TD, Skraba A, Massi R. Design and test of an ironless axial flux permanent magnet machine using Halbach array. Int J Modern Eng. 2014;52.
23. Fleisch D. A student's guide to Maxwell's equations. Cambridge University Press; 2008.
24. Chabu IE, Silva VC, Lebensztajn L (s.d.). Development of the ventricular assist device drive motor. “Desenvolvimento do motor de acionamento do dispositivo de auxílio ventricular”. São Paulo; 2010.
25. Lopes G, Bock E, Gomez L. Numerical analyses for low Reynolds flow in a ventricular assist device. Artif Organs. 2017;41(6):E30–E40.
26. Rodrigues M, Da Cruz NC, Rocha J, Sá R, Bock E. Surface roughness of biomaterials and process parameters of titanium dioxide gritblasting for productivity enhancement. Acad Soc J. 2019;3(2):169–76.
27. da Silva BU, Jatene AD, Leme J, Fonseca JW, Silva C, Uebelhart B, et al. Vitro assessment of the apico aortic blood pump: anatomical positioning, hydrodynamic performance, hemolysis studies, and analysis in a hybrid cardiovascular simulator. Artif Organs. 2013;37(11):950–3.
28. Desaive T, Horikawa O, Ortiz JP, Chase JG. Model-based management of cardiovascular failure: where medicine and control systems converge. Annu Rev Control. 2019. https://doi.org/10.1016/j.arcontrol.2019.05.003
29. DelMonaco A, Hirata MH. Subcloning, expression and purification of Human Hialuronidase-1, variant 8. Acad Soc J. 2019;3(1):50–63.

How to cite this article: de Souza RL, Chabu IE, Drigo da Silva E, de Andrade AJP, Leao TF, Bock EGP. A strategy for designing of customized electromechanical actuators of blood pumps. *Artif Organs*. 2019;00:1–6. https://doi.org/10.1111/aor.13556